A. S. M. Maksud Kamal · Farhad Hossain · Md. Zillur Rahman · Bayes Ahmed⬥ · Peter Sammonds

Geological and soil engineering properties of shallow landslides occurring in the Kutupalong Rohingya Camp in Cox's Bazar, Bangladesh

Abstract The Forcibly Displaced Myanmar Nationals (FDMN), historically known as 'Rohingya' who fled the 2017 ethnic atrocities and genocide in the Northern Rakhine State of Myanmar, took shelter in Cox's Bazar District of Bangladesh. The camp network, known as Kutupalong Rohingya Camp (KRC), is situated in the tectonically active tertiary hilly terrain. The KRC has been experiencing hydrometeorological hazards, where landslides are frequent. This study investigated the slopes' geological condition, engineering properties and human interventions, which influence the landslides. The exposed slopes were relatively high (> 10 m) and steep ranging from 40° to 60° that have numerous polygonal tension cracks and fissures. From the geological and geotechnical aspects, there are three successive units of slope materials: (1) residual soils of sandy silt with clay, (2) highly weathered silty sandstones and (3) shale/clay with silt and fine sand intercalations at the bottom of the slopes. Field observations revealed that most slope failures occurred in the residual soil and weathered silty sandstone units. The residual soils have a bulk density of 1.49–1.97 g/cm³, a liquid limit of 25–48%, a plasticity index of 5–16% and an undrained shear strength of 23–46 kPa. The silty sandstones have a bulk density of 1.44–1.94 g/cm³, an internal friction angle of 34°–40° and a cohesion of 0.5–13 kPa. The mineralogical composition determined by the X-ray diffraction shows low clay mineral content, which does not affect landslides. However, the slope geometry, low shear strength with strain softening properties and torrential rainfall accompanied by anthropogenic factors cause numerous landslides every year. This study will help take proper mitigation and preparedness measures for slope protection in the KRC area and surroundings.

Keywords Rohingya · Landslides · Geology · Soil engineering · Anthropogenic factors · Cox's Bazar

Introduction

In the tectonically active and hilly areas, rainfall and earthquake-induced landslides are common phenomena worldwide. Landslide-prone slope poses a threat to human life, livelihood, critical infrastructure and ecosystem (Highland and Bobrowsky 2008). In 2017, following the ethnic violence and genocide in the Rakhine State of Myanmar, about a million 'Forcibly Displaced Myanmar Nationals (FDMN)' popularly known as the 'Rohingya' were forced to flee across the border into Bangladesh. The displaced Rohingyas took shelter in the hilly terrain, located in the south-eastern Cox's Bazar District, known as Kutupalong Rohingya Camp (KRC). Thousands of temporary shelters were built to accommodate the Rohingyas in the entire area by removing and destroying the forest

and vegetation cover. This act has increased weathering and erosion rates, which ultimately caused thousands of small-scale shallow landslides (Zaman et al. 2020).

During the 2020 monsoon season (June to October), around 5580 refugees were affected by 638 slope failures, another 710 wind/storm and 31 flooding events in the camp area (ISCG 2020). Landslides in this area/region have been studied in terms of spatial susceptibility zoning (Ahmed 2015; Tehrani and Husken 2019), geospatial mapping (Braun et al. 2019; Hasan et al. 2020), community vulnerability assessment (Ahmed 2021; Sultana 2020), risk-sensitive land use planning (CDMP-II 2012) and rainfall threshold determination and hydrometeorological early warning system development (Ahmed et al. 2020). Low shear strength, dispersive behaviour of soil due to the high clay content and intense seasonal rainfall coupled with anthropogenic activities were identified as the leading causes of landslides in the region (Ahmed 2021; Highland and Bobrowsky 2008). Nevertheless, the magnitude of geological processes, the engineering properties of the hillslope materials and human activities causing slope failure are yet to be studied in depth.

Engineering properties of landslide materials are fundamental to determine which factor will be favourable to produce landslides and the extent of a specific type of landslide (Uyeturk et al. 2020; Zhan et al. 2019). For example, soil landslide has shallow scarps, whereas bedrock landslide has deeper scarps (Michel et al. 2020). The type of landslides, such as fall, slide, and flow, also depends on the soil properties. To overcome such limitations, this study aims to (a) determine the underlying geological mechanism and earth surface processes, (b) investigate the soil engineering properties of slope materials and (c) evaluate the effects of the mineralogical and chemical composition of slope failure in the KRC area.

The Kutupalong Rohingya Camp

Study area profile

The KRC covers a 14.6-km² area of Ukhia Upazila (sub-district) in the south-eastern part of Cox's Bazar District, Bangladesh (Fig. 1a, b). There are about 23 camps within the KRC area (Fig. 1c). As of February 2021, the total Rohingya population of the KRC area was about 615,000, with a density of 42,000 people/km² (GoB-UNHCR 2021). The Rohingyas are living in numerous temporary shelters located in the foothills, slopes and flat hilltops. Oblique subduction and collision between the Indian and the Burma plates have produced the N-S trending Indo-Burma range where the KRC is situated (Curray 2005). Elevation in the area ranges from about − 5 to 38 m.
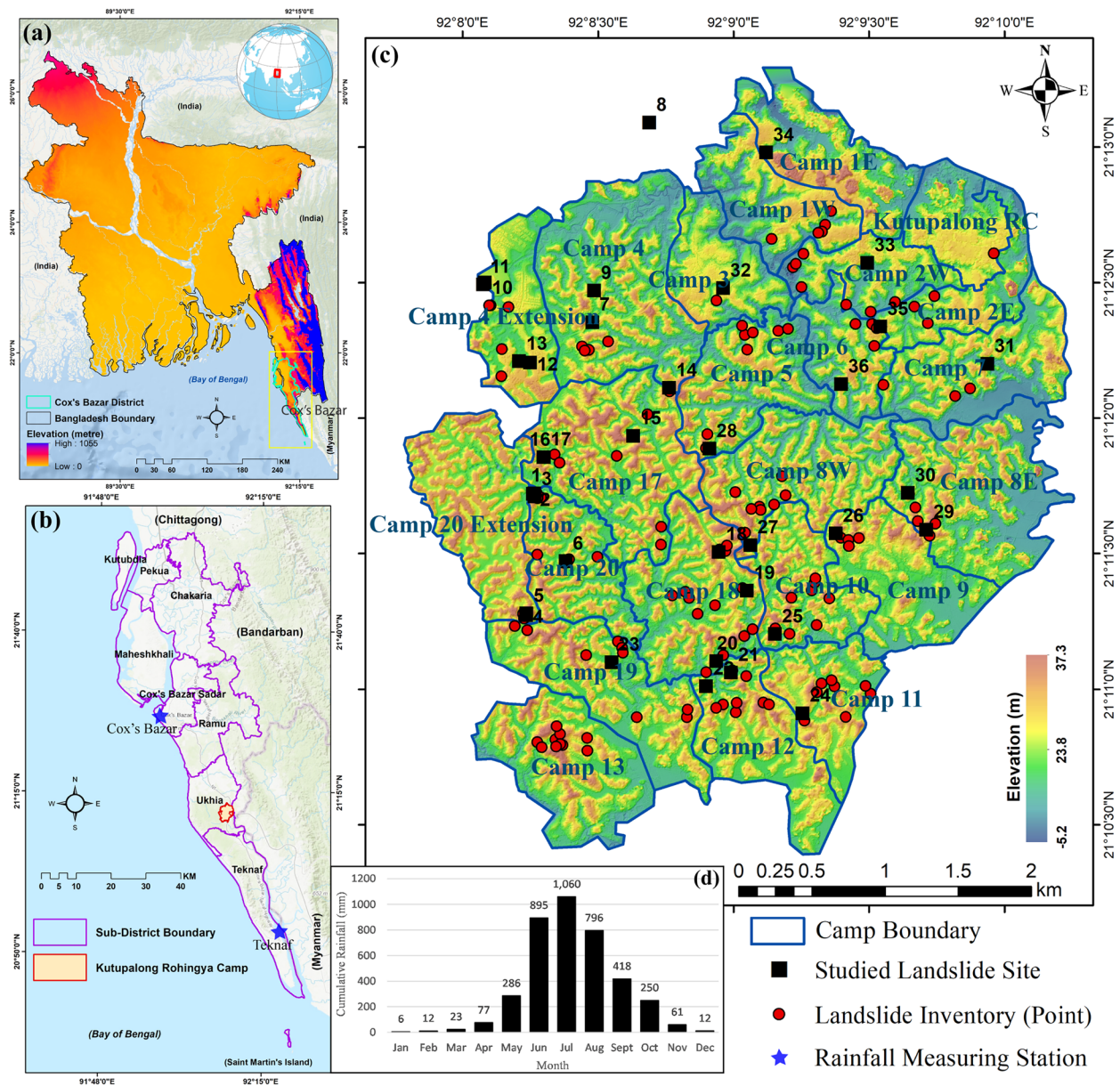
Fig. 1 The location of the study area and sampling points. **a** Location of Cox's Bazar District in Bangladesh. **b** Sub-district of Cox's Bazar with rainfall measuring station locations. **c** Elevation map of Kutupalong Rohingya Camp and sampling point locations. **d** Average monthly rainfall distribution from Cox's Bazar and Teknaf stations

The regional geology of this area is composed of Miocene to Recent aged clastic sedimentary rocks. The Miocene and Mio-Pliocene Bhuban (Tb) and Boka Bil (Tbb) formations are predominantly composed of alternating sandstones and shales. The Pliocene Tipam (Tt), Plio-Pleistocene Girujan (QTg) and Pleistocene Dupi Tila (QTdt) formations are composed of massive fluvial sandstone, lacustrine clay and unconsolidated fluvial sandstone deposits, respectively. The recently aged alluvium (ava) and marshy clay and peat (ppc) overlain the Pleistocene-recent Dihing (QTdi) Formation along with the broad synclinal valley areas (Fig. 2a).

The KRC area sits between the Olatang and Inani anticlines along a broad syncline valley (Fig. 2b). The loose Dupi Tila,

Girujan Clay and Tipam formations are exposed in the KRC area, which is affected by strong weathering and erosional phenomena. The area has a moderate thick (~2–5 m) surface soil that covers the partially or wholly weathered loose bedrock (Reimann and Hiller 1993). The KRC area comprises many low-rounded hills, hillocks and valleys covered with dense forests and shrub vegetation (Hasan et al. 2020; Reimann and Hiller 1993). The highest average monthly cumulative rainfall is observed, around 1000 mm in July, and the lowest rainfall occurs in January and December, about 6 mm and 12 mm, respectively (Fig. 1d). The average temperature of the area is about 25.6 °C (Zaman et al. 2020).
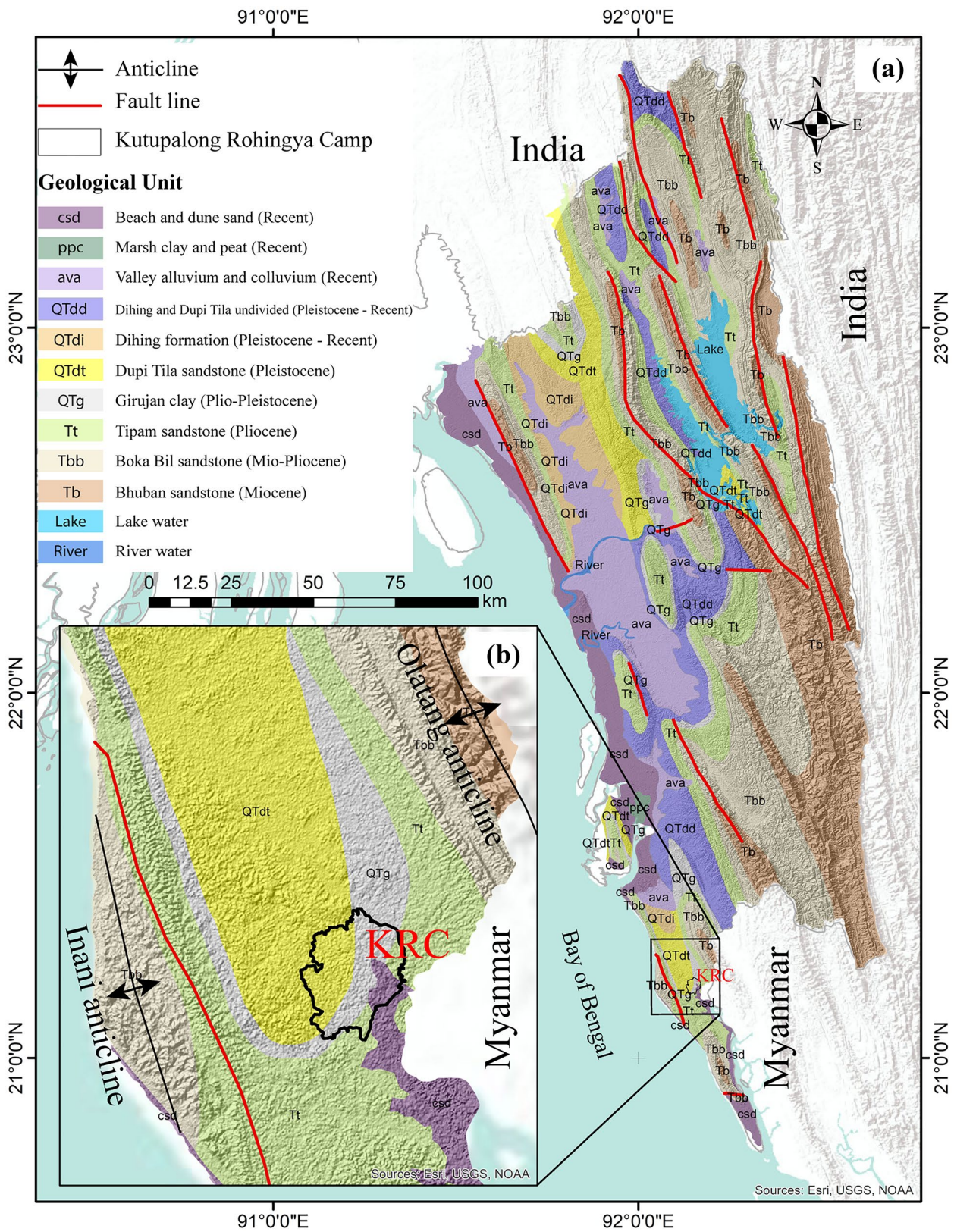
Fig. 2 **a**, **b** Tectonic and regional geological setting of the Chittagong hill district (CHD) region, adapted from Persits et al. (2001)

Land use scenario of the KRC area

The displaced Rohingyas have been living in fragile shelters that are highly vulnerable to natural hazard-induced disasters. The shelters were built very densely without keeping sufficient open space, which creates a chaotic environment for them to live in (Alam et al. 2020). The average usable space is only 10.7 m² per person at KRC. Before the Rohingya settlement, the land use types of this area were mainly agriculture, forest and vegetation, with a minor settlement of the present host community.

Due to the Rohingya influx, significant land cover changes were observed in the Ukhia and Teknaf sub-districts of Cox's Bazar. About 5100 ha of vegetated land, 1000 ha of water bodies and 450 ha of barren (sandy) land were destroyed (Hossain and Moniruzzaman 2021). From the decreased vegetated land in the present study area, about 20% was used for camp expansion. The other 80% was deforested for transportation and other utilities for the Rohingya community (Braun et al. 2019; Hasan et al. 2020).

At several locations within the camp area, the slopes are highly prone to slides soon as creep and polygonal tension cracks are observed on the crest of the slopes (Fig. 3). Around 30% and 17% of the KRC areas are highly susceptible to flooding and landslides, respectively (Zaman et al. 2020).

Methodology

Fieldwork and sample collections

A comprehensive fieldwork from 26 November to 12 December 2020 was carried out to examine the landslide potential of the exposed slope materials of the KRC. The disturbed and undisturbed samples of partially decomposed parent rock materials and the soil samples were collected from the main body, sliding mass and substrate (Fig. 4a) to determine their mechanical properties in the laboratory. In total, 151 landslide locations were identified, and out of which, 36 sites (Fig. 1c) were investigated in-depth, considering the slope failures' fresh slope morphology, easy accessibility and disaster risk severity. From the geological point of view, the morphology, materials (i.e. soil or rock) and sliding behaviour of landslides were briefly investigated.

For the determination of in situ density and unconfined compressive strength (UCS), undisturbed/partly disturbed samples were collected from the main body/substrate of landslide by inserting steel core barrel into the soil with a dimension of 3.8 cm diameter and 10 cm length and were weighed immediately after collection in the field (Fig. 4b). For the direct shear test, samples were collected using an 8-cm-diameter and 14-cm-long PVC pipe. The disturbed sample from sliding mass was collected and carried

Fig. 3 Landslides in the Kutupalong Rohingya Camp (photos taken during the fieldwork). **a** Camp 18 (slump). **b** Camp 4 (rotational slide). **c** Camp 20 (creep with polygonal tension cracks). **d** Camp 17 (slump/debris flow). **e** Camp 8E (slump). **f** Camp 5 (rotational slide)

Fig. 4 Fieldwork photos. **a** Outcrop section of a landslide. **b** Soil core sample drilled from the landslide site in the KRC area
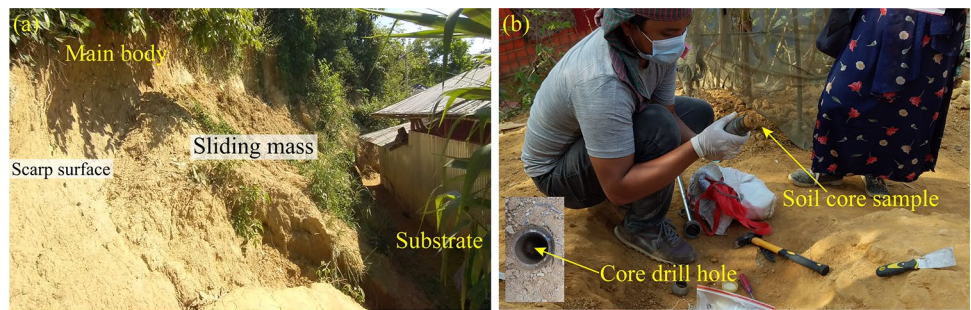
by zipper plastic bags. The disturbed samples were used for grain size analysis, Atterberg limits and specific gravity determination.

Laboratory experiments

A series of laboratory investigations were conducted to determine the soil engineering properties of the hillslope materials collected from the KRC area following the ASTM standards (ASTM 2020a, 2020b).

Basic soil properties

The primary soil engineering properties of the samples collected from KRC were investigated for the preliminary assessment of the ground condition and slope failure. For moisture content determination, 50 g of soil was placed in a porcelain dish and heated in an oven of 110 °C temperature for about 12 h for each sample. The organic content was determined by burning 50 g soil of each sample in a muffle furnace at 440 °C around 12 to 14 h (Hoogsteen et al. 2015; Uyeturk et al. 2020). To measure the specific gravity of each soil sample, a 250-ml flask (water pycnometer) was filled with water, and 50 g of soil passed through the 4.75-mm sieve. A pH meter calibrated by pH 4.00 and 7.00 standard buffer solution was used to measure soils' acidic/alkaline state. For soil classification, grain size analysis and Atterberg limits (liquid and plastic limit) were determined. During the hydrometer analysis, 152H hydrometer and sodium hexametaphosphate as a dispersing agent were used. The liquid limit (LL) and plastic limit (PL) were also determined for the soil samples using a Casagrande cup following ASTM D4318-17 standard. The plasticity index (PI), which is the difference between the liquid limit and the plastic limit, was also measured.

Unconfined compressive strength test

The UCS was determined for 18 suitable fine-grained cohesive soil and shale/clay samples to understand the undrained strength of the material under maximum uniform axial stress. The ASTM D2166/D2166M-16 standard was followed to perform the test. For this test, soil samples drilled by steel core barrels were trimmed to 38 mm diameter and 80 mm height. After that, a uniform axial strain rate of 0.6 mm/min was applied to the specimen. In this process, a continuous load was applied until the load dial reading decreased with increasing strain or the attainment of 15% strain.

Direct shear test

A total of 12 soil samples was tested using direct shear equipment for determining consolidated drained shear strength properties according to ASTM D3080-04 standard. Samples were then placed in a 6-cm square shear box having 2 cm thickness. Afterwards, 55 kPa, 110 kPa and 220 kPa normal loads were applied for three consecutive tests, as the soils in the field condition were exposed to high vertical loads.

Identification of soil mineralogy

For this particular investigation, five characteristic soil samples randomly distributed in the KRC area were tested largely to know their mineralogical compositions and influence on landslide occurrence and weathering phenomena. First, X-ray diffraction (XRD) analyses were conducted in the powdered soil samples at the diffraction angles of 3° to 70° 2θ CuKα in air-dried condition. Then, the same sample was treated with ethylene glycol and heated at 550 °C, and tested again for confirming the identified clay minerals (Hillier 2009). The morphology and structure of the minerals were also studied using the scanning electron microscope (SEM).

Results and discussion

Geology and hillslope process of landslides

The exposed slope materials of the KRC area can be classified into three generalized stratigraphic successions. These layers consist of (a) three stratigraphic layers as residual soil–silty sandstone–shale/clay (Fig. 5a, a′), (b) two stratigraphic layers as residual soil–silty sandstone (Fig. 5b1, b2, b′) and (c) one distinct silty sandstone column with little or no soil cover (Fig. 5c, c′). Most of the exposed slopes in the study area are steep, ranging from 40° to 60°, whereas the height ranges from 10 to 15 m.

During the monsoon, the infiltrated rainwater passing through the upper soil layer flows with higher velocity in the underlying sandstone unit due to its higher porosity and permeability. The pore water pressure due to the preferential flow in the sandstone reduces the effective stress that results in shear strength reduction. The washing and leaching of the clay materials that bind the coarse-grained sand particles also contribute to the shear strength reduction of the sandstone layer. The rainwater that flows through the sandstone layer forms seepage at the base of the slope (Fig. 5a′, b′, c′). After the initiation of slope failure on the toe or base of the slope, it propagates or advances towards the higher elevation with the retrogressive pattern of landslide. Consequently, the same slope fails every year during the rainy season. The morphological features of landslides, such as scarp surface or sliding plane, toe and head or crown with polygonal tension cracks, are visible (Fig. 5a, b1, b2, c) in the KRC area. Slope failures in the KRC area are primarily of the rotational slide and slumping type (Fig. 5a′, b′, c′). Where the soil

Table 1 Index properties of the soil (landslide material) samples

Site no.[a]	In situ bulk density (g/cm³)	In situ moisture content %	pH	Specific gravity, Gs	Organic content (%)	LL (%)	PL (%)	PI (%)	USCS	Geotechnical (stratigraphic) unit
1	1.96	26.53	3.0	2.55	4.74	50	31	19	ML/MH	SCU
2	1.44	10.99	3.9	2.64	2.48	–	–	–	SP-SM	SSt
3	1.97	16.44	3.6	2.59	4.79	34	21	13	SC (CL)[b]	RS
4	1.52	17.22	4.3	2.67	1.40	–	–	–	SP-SM	SSt
5	1.88	26.33	3.3	2.59	4.32	48	32	16	ML	RS
6	1.83	30.08	4.4	2.63	4.83	43	27	16	ML	SSt
7	1.90	28.09	3.2	2.59	3.89	33	23	10	CL	RS
8	1.81	36.25	3.9	2.62	3.05	33	25	8	ML	RS
9	1.94	22.53	4.0	2.56	4.29	29	22	7	SP-SC (CL)[b]	SSt
10	1.98	31.15	3.3	2.54	4.52	52	30	22	MH	SCU
11	1.45	13.49	3.8	2.67	1.95	37	25	12	ML	SSt
12	1.92	26.17	3.1	2.62	4.53	36	26	10	ML	RS
13	1.74	20.29	3.5	2.56	4.82	31	23	8	ML	RS
14	1.49	11.42	4.5	2.75	3.73	45	29	16	ML	RS
15	1.74	21.97	3.3	2.53	6.10	–	–	–	SM	SSt
16	1.64	8.90	4.2	2.61	2.56	40	28	12	SM (ML)[b]	SSt
17	1.55	10.20	4.3	2.55	4.11	38	24	14	SM (CL)[b]	SSt
18	1.89	25.29	3.9	2.62	5.83	–	–	–	SM	SSt
19	1.82	14.22	4.2	2.62	4.20	27	22	5	SC-SM (ML)[b]	SSt
20	1.67	15.42	4.2	2.58	3.45	36	21	15	CL	RS
21	1.64	12.01	4.4	2.62	3.76	44	25	19	SC-SM (CL)[b]	SSt
22	1.75	16.87	3.5	2.60	4.92	40	27	13	ML	RS
23	1.76	12.34	3.4	2.62	3.71	–	–	–	SM	SSt
24	1.58	12.91	3.7	2.56	4.37	36	26	10	ML	RS
25	1.85	11.04	3.6	2.57	2.91	34	24	10	SM (ML)[b]	SSt
26	1.72	15.37	3.8	2.63	3.34	56	37	19	SM (MH)[b]	SSt
27	1.65	19.75	3.6	2.51	5.39	39	28	11	ML	RS
28	1.66	17.31	4.5	2.51	4.35	38	26	12	ML	RS
29	1.71	14.83	3.9	2.62	4.35	38	22	16	SC-SM (CL)[b]	SSt
30	1.72	14.50	3.8	2.61	3.90	30	21	9	SC-SM (CL)[b]	SSt
31	1.90	21.09	3.9	2.60	6.01	31	19	12	CL	RS
32	1.81	16.98	3.6	2.61	4.63	34	24	10	ML	RS
33	1.80	18.44	3.9	2.59	4.69	32	20	12	CL	RS
34	1.78	26.02	3.8	2.61	6.20	42	28	14	ML	RS
35	1.63	20.28	4.4	2.56	5.62	39	26	13	ML	RS
36	1.81	22.95	3.5	2.62	5.57	25	20	5	CL-ML	RS

SCU shale or clay unit, *SSt* silty sandstone, *RS* residual soil

[a] Site no. indicates the location of the sample in Fig. 1

[b] The Atterberg limits are determined for the fine portions only, and associated soil classification is within the brackets

Table 2 The unconfined compression test results of undisturbed soil samples collected by tube core barrel

Sample no. (site no.)	Average water content (%)	UCS (kPa)	Strain at failure (%)	S_U (kPa)
U-1–1 (1)	26.48	102.32	6.41	51.16
U-1–2 (3)	–	59.52	3.57	29.76
U-2–1 (5)	31.68	75.78	3.32	37.89
U-3–1 (7)	27.71	49.08	4.51	24.54
U-3–2 (8)	20.94	70.4	2.26	35.20
U-4–1 (10)	34.52	81.32	4.90	40.66
U-4–2 (12)	29.33	88.84	4.93	44.42
U-6–2 (20)	19.70	57.22	2.26	28.61
U-7–1 (23)	17.53	81.6	3.69	40.80
U-8–1 (24)	30.94	85.44	4.22	42.72
U-8–2 (25)	19.71	66.4	2.45	33.20
U-9–2 (28)	26.27	92.76	2.41	46.38
U-10–1 (30)	18.30	70.3	1.31	35.15
U-10–2 (31)	21.18	61.24	2.02	30.62
U-11–1 (33)	20.21	52.58	5.03	26.29
U-11–2 (34)	34.48	59.16	4.14	29.58
U-12–1 (35)	26.10	46.46	2.04	23.23
U-12–2 (36)	25.23	83.28	2.63	41.64

layer has a considerable thickness (> 4 m), the slumping features, e.g. multiple heads and stair-step patterns, are well developed. The depth to which soils are developed can affect the volume of material eroded and ranges from several vertical meters in deep rotational or translational landslides to several centimetres in recent, shallow soils (Fort et al. 2010).

Three types of human activities were observed in the KRC area: excavating the toe, loading the slope by shelter constructions and removing forest cover. Due to the construction of shelters and associated camp facilities, the slope materials were excavated indiscriminately from its toe or base. In addition, the loss of root cohesion due to widespread deforestation also decreases the shear strength and increases the weathering of the slope materials. The state of weathering of a rock mass has a significant influence upon its strength, permeability and ease with which its material may be deformed. Hence, weathering processes affect the sliding resistance of the slope materials. Furthermore, the weight of the overburden due to constructions of shelter houses on top of the slope increases the downslope stress causing the development of the tension cracks at the crown and around (Fig. 3). The above observations revealed that the combined effects of near-surface geology, hillslope processes and anthropogenic interventions reduce the shear strength of the slope materials of the KRC area, which trigger landslides during the monsoon season (June–October).

Index properties of soil

The index properties of the soil samples, viz. in situ bulk density and moisture content, organic content, Atterberg limits (LL, PL, PI), specific gravity and pH, are presented in Table 1. The in situ density of the bulk soil sample was determined for all the locations of landslides, where the maximum, minimum and mean values of soil density were found to be 1.97 g/cm³, 1.44 g/cm³, and 1.75 g/cm³, respectively.

A relatively high bulk density represents high compaction but a low porosity of the soil. A lower density value was observed in the loosely consolidated sandstone, whereas uniform clay has the highest density. The moisture content of the soil samples determined in the field varies from 8.9 to 36.25%, with an average of 19%. The laboratory-determined moisture contents have a similar result as the in situ condition and are shown in Tables 2 and 3. The estimated pH values ranged from 3 to 4.5, with an average value of 3.8, which indicates a strongly acidic environment. Soil pH is affected by the mineral composition of the soil's parent material
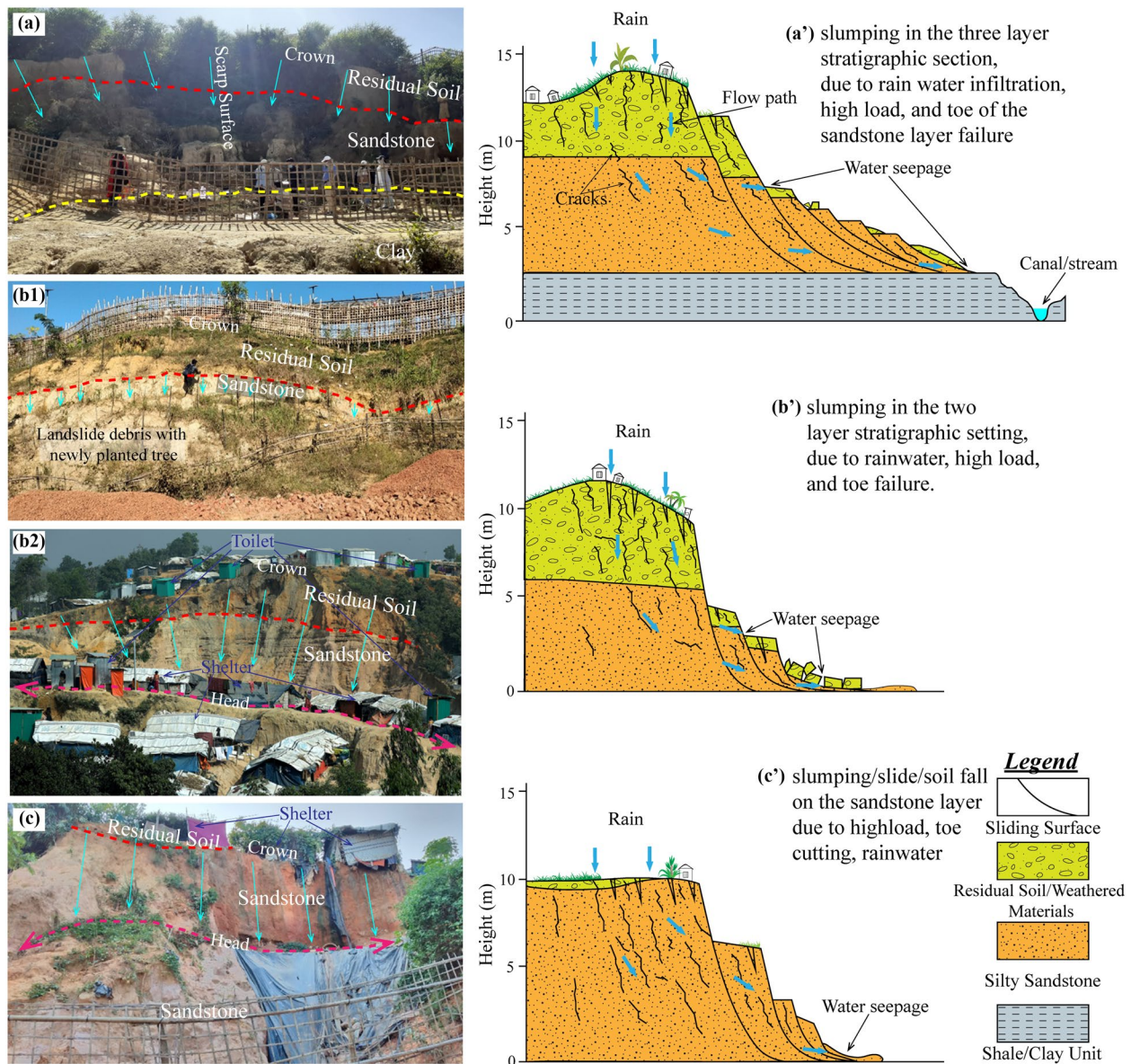
Table 3 The direct shear test results of the undisturbed soil samples

Sample no. (site no.)	Lithology	Average initial water content (%)	c' (kPa)	φ' (°)
DS-1–1 (2)	Medium to fine sandstone	9.5	0.50	39.87
DS-2–1 (4)	Medium to fine sandstone	5.7	1.67	38.31
DS-2–2 (6)	Fine sandstone	20.7	10.42	34.33
DS-3–1 (9)	Medium to fine sandstone	4.5	2.08	38.20
DS-4–1 (11)	Fine sand to silt	12.5	8.75	39.18
DS-5–3 (15)	Medium to fine sandstone	32.5	2.09	38.65
DS-5–4 (16)	Silt to clay	14.7	7.08	38.58
DS-6–3 (22)	Fine sandy soil	13.7	10.67	37.66
DS-7–2 (23)	Fine sand to silt	10.6	11	34.94
DS-10–1 (29)	Fine sandstone	8.7	13.33	36.35

Fig. 5 Exposed outcrops of the shallow landslides (slumping) and corresponding schematic geological cross sections in the KRC area. **a** Three stratigraphic layer, **b** two-layer and **c** one-layer controlled landslides

and the weathering reactions undergone by that parent material (Bloom 2020). The acidic pH of the soil of the study area indicates sizeable internal water drainage–dominant weathering in the study area. The specific gravity of all the samples ranged from 2.51 to 2.75, with an average value of 2.59. In silty soil, the specific gravity was found to be 2.5–2.6, representing a slightly lower value than silt's ideal specific gravity (2.70). This phenomenon is attributed to the organic matter in silty soil (Gui et al. 2021). The organic content of the tested soil samples was in the range of 1.4 to 6.2%, with an average value of 4.25%.

Soil classification

As mentioned, wash sieve and hydrometer analyses were used to determine the grain size distribution of the studied soil samples. Data obtained from both sieve and hydrometer analysis are plotted in a single graph of particle size vs. cumulative percentage of soil particle (Fig. 6). The grain size distribution curve and percentage of sand, silt and clay are illustrated in Fig. 6, showing that the percentage of sand, silt and clay grained particles is 12.7–93.92%, 4.58–68.3% and 0.7–28%, respectively. The results showed that out of 36 samples, 15 represent

Fig. 6 **a** The cumulative grain size distribution curve and **b** proportion of sand, silt and clay
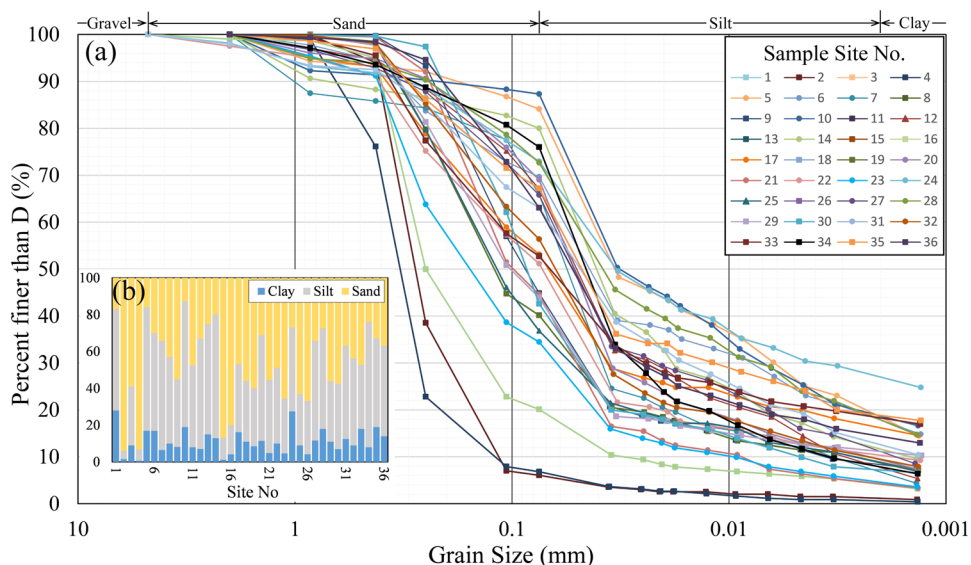
coarse-grained soils and are classified according to the Unified Soil Classification System (USCS) nomenclature (Table 1). The coarse-grained soils mostly belonged to silty sand (SM); few were classified as clayey sand (SC) and mixed silty clayey sand (SP-SC/SC-SM).

The remaining 21 fine-grained soils (50% or more soil particles passing through the no. 200 sieve) were classified by determining their Atterberg limits, i.e. LL, PL and PI. The LL, PL and PI determined for 21 fine-grained soil samples were between 25 and 52%, between 19 and 32% and between 5 and 22%, respectively (Table 1). The LL and PI values are plotted in the plasticity chart (Fig. 7), which indicates that most of the samples tested consisted of silt and lean clay type soils. A few of them are elastic clay and silty clay; no fat clay was found (Table 1). Among the 21 fine-grained soils, 15 were classified as silt (ML), while 4 lean clay (CL), 1 elastic silt (MH) and 1 silty clay (CL-ML) were found. The Atterberg limits of the fine portion of the coarse-grained soils were also determined and are shown in Table 1.

Unconfined compressive strength

The undrained shear strength (S_U) of the fine-grained soil samples obtained by the UCS test is shown in Table 2. The average shear strength value is 36 kPa, whereas the maximum value is estimated at 51.16 kPa at site location 1 in camp no. 20. This sample is collected from the lower clay layer as shown in Fig. 5a′. The lowest undrained shear strength found in the UCS test is about 23.23 kPa. The minimum UCS value is observed at the coarse particle mixed fine soils. During the UCS test, soil samples in some cases show straight shear failure planes but, in some cases, rugged irregular surfaces, and some also show bulging at the failure (Fig. 8). It may be due to the inclusion or mixture of different size particles and relatively less tight packing. The axial strain vs. stress curve represents that deformation of the soils occurred at the falling strain ranging from 1.31 to 6.41% (Fig. 9). Most of the soil samples during the UCS test show strain-softening

Fig. 7 The plasticity chart of Atterberg limit values (legends are in Fig. 6)
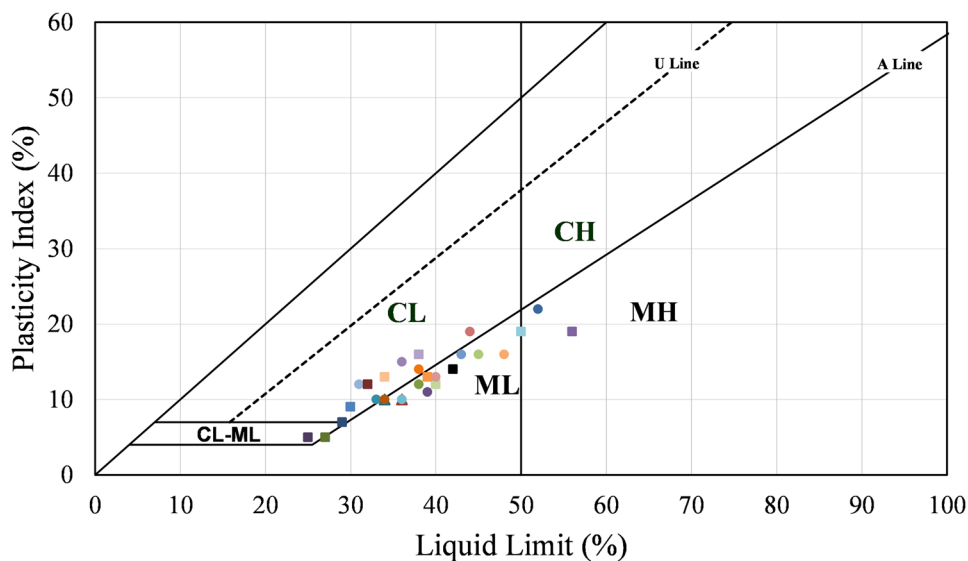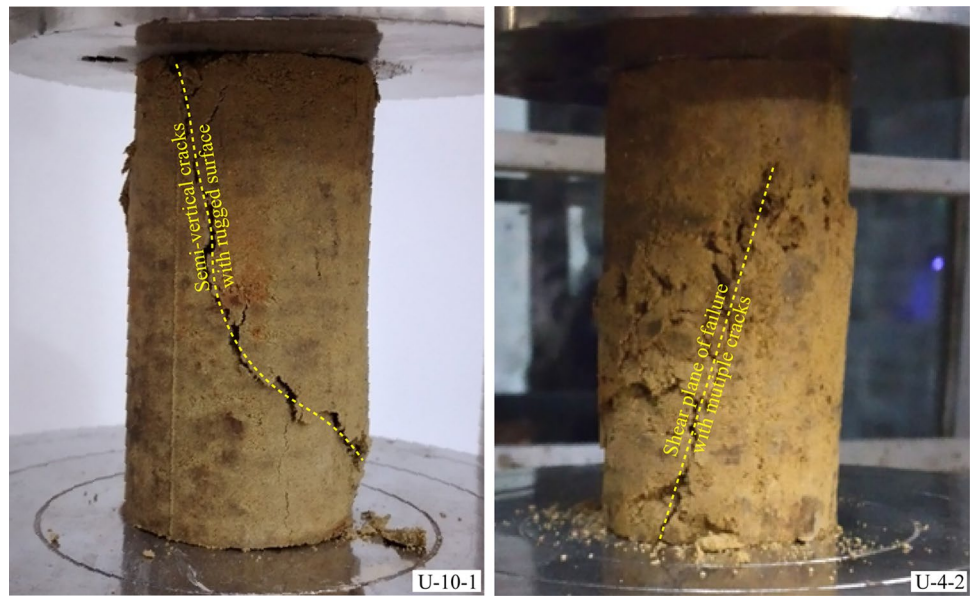
Fig. 8 Typical shear failure pattern observed in the UCS test

behaviour, and also some of them deformed plastically (Fig. 9). Soils with densely packed grains are strain softening because disturbance during sharing causes the grains to move apart, causing dilation (Davison and Springman 2000). The slopes which composed of fine-grained particles are well suited to develop landslide shear surfaces due to their strain softening property at the KRC area.
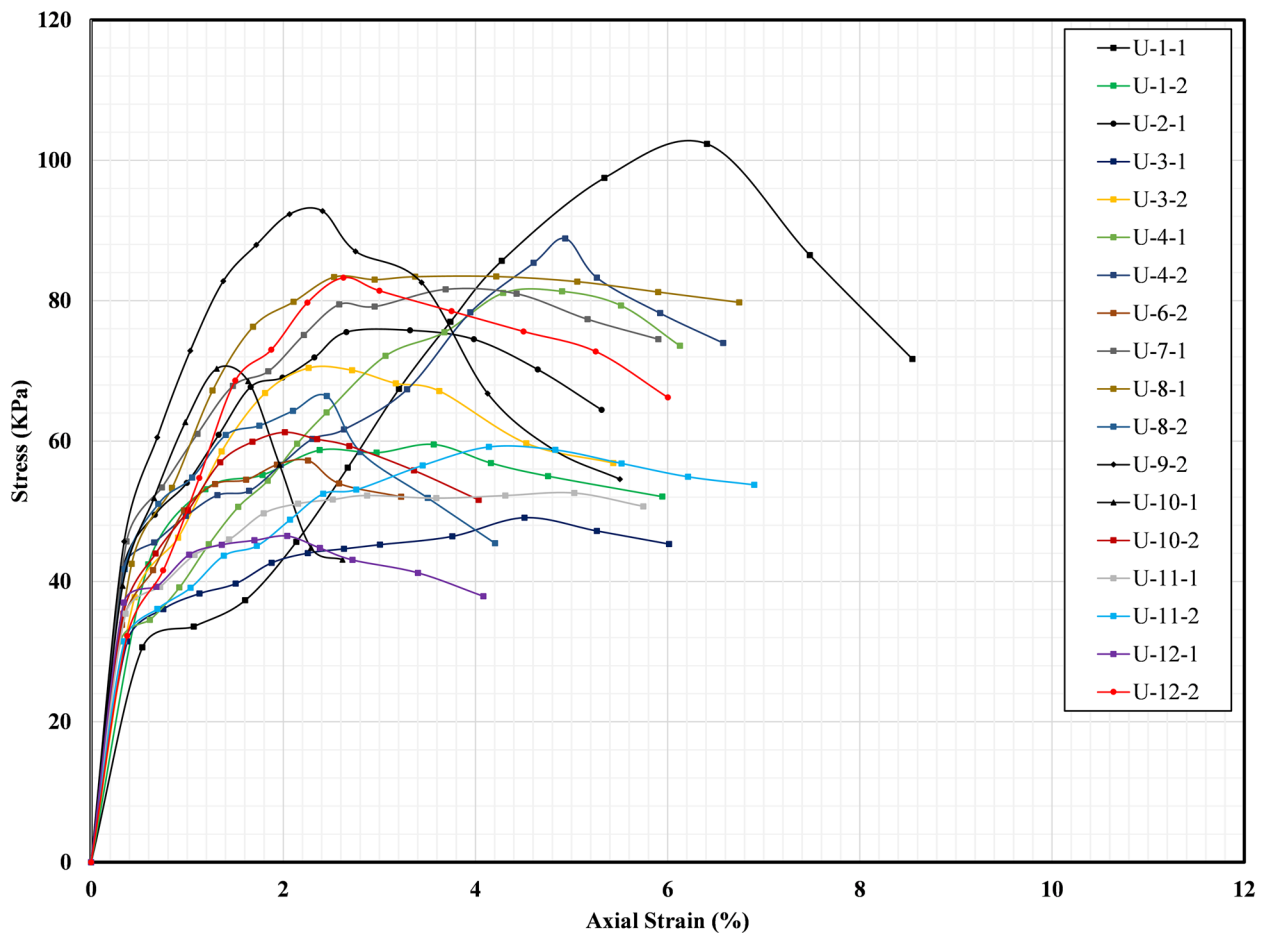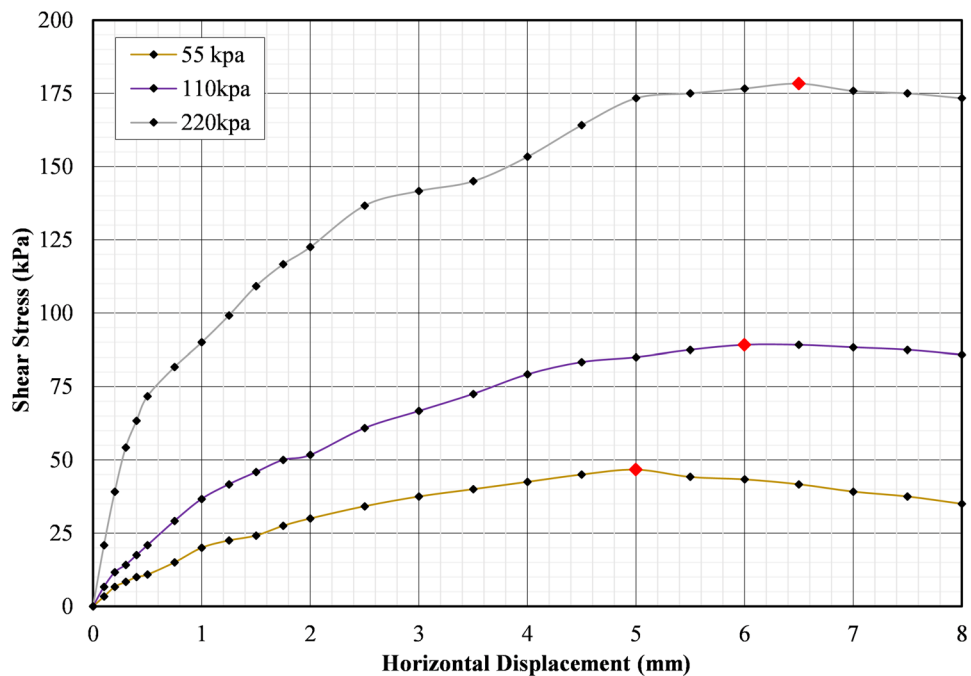

Fig. 9 The stress–strain behaviour of soil in the unconfined compression test

Fig. 10 The shear stress vs. horizontal displacement plot of a representative soil sample (DS-5–3) in the direct shear test. Red rectangle indicates peak resistance

Direct shear test

The coarse-grained soils are tested to evaluate their shear strength parameters. The cohesion and friction angle results obtained from the direct shear test for ten samples are shown in Table 3.

The shear stress is applied until 8-mm horizontal displacement occurs, and all the samples show ultimate resistance to applied stress within this limit. The horizontal displacement vs. shear stress behaviour of a characteristic soil sample is shown in Fig. 10. The obtained cohesion and friction angles range from 0.5 to 13.33 kPa and from 34.33° to 39.87°, respectively (Table 3). Friction angles are found higher for relatively sandy soils, whereas clayey soils

represent higher cohesion values. The samples tested in the direct shear equipment have shallow water content, which gives the actual shear strength of the material properties without the influence of pore water. When all the direct shear test data are plotted in a single graph, the shear envelope has an average cohesion value of 6.75 kPa against the friction angle of 37.64° (Fig. 11).

Mineralogical composition

The XRD analyses of five soil samples (sites 12, 20, 24, 31 and 36) randomly distributed over the camp area were carried out to determine the mineralogical composition of the fine-grained upper soil.

Fig. 11 The shear stress vs. normal stress plot of all the direct shear test data showing an average trend of internal friction angle and cohesion

$$y = 0.7714x + 6.7592$$
$$R^2 = 0.9865$$
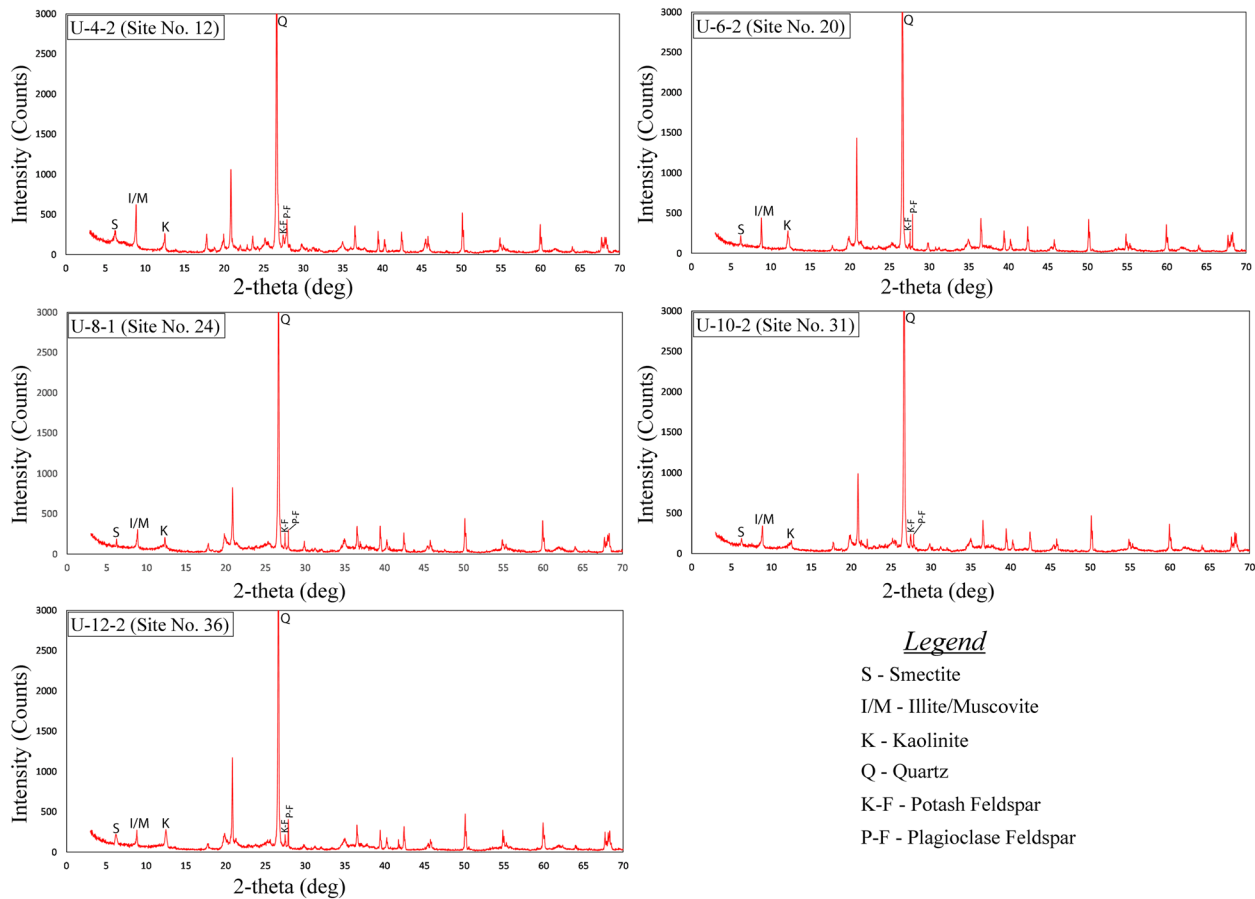
$\varphi = 37.64°$

$c = 6.75$ kPa
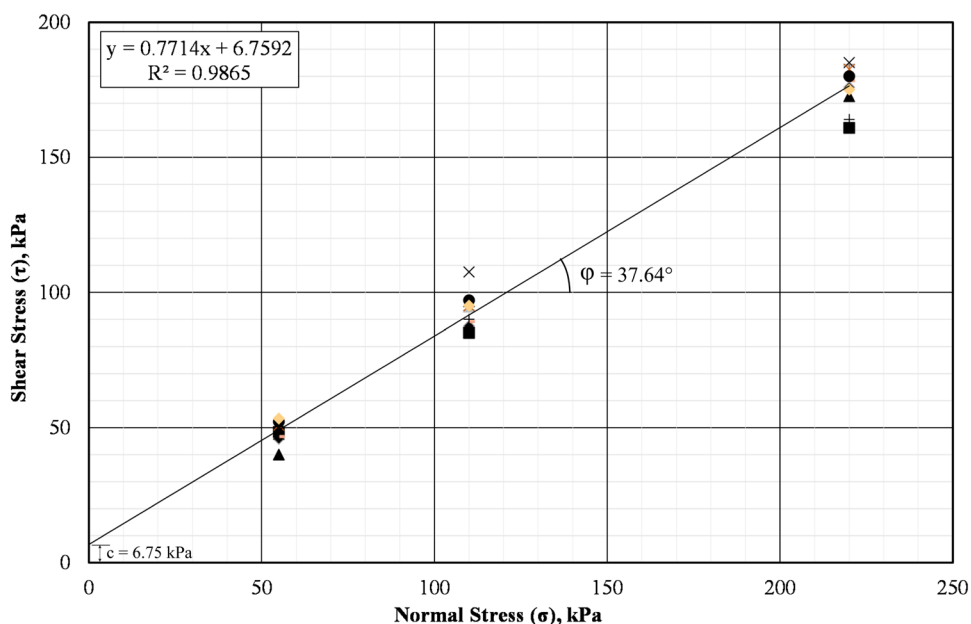
Fig. 12 Mineral composition of the soil samples derived by the X-ray diffraction (XRD) analysis

The XRD spectral characteristics of the investigated samples are shown in Fig. 12. The mineralogical abundance is dominated by quartz (> 60%), feldspar (4–7%) and clay minerals. Clay minerals consist of kaolinite (3–5%), illite/muscovite (8–10%) and smectite (< 2%). In some soil samples, abundance of clay minerals is trivial. The threshold for the swelling or expansion potentiality of clay is indicated by more than 10% clay, while more than 30% clay content exhibits extreme expansion potential (Kariuki and van der Meer 2004). Clay percentage and swelling clay minerals (montmorillonite and smectite) are present in a minimal amount so their impact on landslides is not significant in the camp area. The low amount of clay minerals also indicates that the slope materials' chemical weathering is trivial in the camp area. Large quantities of quartz in the fine-grained portion of the soils indicate a dominant physical weathering process in the KRC area.

Conclusion

The slope materials of the Kutupalong Rohingya Camp (KRC) area are categorized into three geotechnical (stratigraphic) units based on geological and geotechnical characteristics. The units are as follows: (1) residual soils on the top, (2) highly weathered silty sandstones in the middle and (3) shale/clay with silt and fine sand intercalations at the bottom of the slopes. Stratigraphically, these geotechnical units belong to the Plio-Pleistocene Dupi Tila

Sandstone Formation. The rainfall-triggered landslides occurred in the residual soils and underlying highly weathered silty fine- to medium-grained sandstones when the adequate shear strength of these geological materials is reduced due to increased pore water pressure during the torrential rainfall in the rainy season. Due to anthropogenic interventions, the infiltration rate of the exposed residual soils is increased due to cracks and fissures developed on the ground surface. As the residual soils and sandstones' void ratio/porosity and permeability are remarkably high, the infiltrated water first flows vertically through the pore spaces, cracks and fissures. When impermeable clay or shale beds are present below the residual soils and weathered sandstones, the pore water flows along the bedding planes whose dip directions are along the slope. As a result, the effective stress along the impermeable bedding planes is reduced to almost zero due to excess pore water pressure that leads to landslides. The steep slope more significant than the internal friction angle (35°–40°) of the slope materials is also a contributing factor to the landslide in the area.

The acidic pH level and occurrence of kaolinite clay minerals in the soil indicate rapid internal drainage of water through the residual soil and underlying sandstone layers (Bloom 2020; Townsend 1985). Therefore, the acidic pH of the soils and the presence of kaolinite clay minerals indicate the prevailing physical weathering conditions of the slope materials that also enhance the occurrence

of landslides. The low to medium PI values (5–22%) indicate the low consistency of the slope materials that increase the infiltration of the rainwater (Wagner 2013). The low undrained shear strength (23 to 46 kPa) of the residual soils indicates soft to medium stiffness and strain softening of the slope materials (Wagner 2013), which contribute to the occurrence of landslides. The effective cohesion (c') and internal friction angle (φ') values are in good agreement with the shallow landslide materials studied in Turkey (Uyeturk et al. 2020), China (Zhan et al. 2019) and India (Prakasam et al. 2020). The effect of soil mineralogy, i.e. the low content of clay, has no effects on landslides. Nevertheless, the leached surface of feldspar seen on SEM indicates the chemical weathering environment at the slope materials. In the deltaic soils of the Bengal Basin, illite, mica and kaolinite are the dominant clay minerals (Ito and Wagai 2017), which support the finding of this study.

Overall, based on the information from the geological and soil engineering property studies, it is observed that the slope geometry, the low shear strength of the slope materials with strain softening properties, torrential rainfall and massive loading accompanied with slope base cutting result in numerous landslide occurrences in the KRC area. The data presented in this study will contribute to understanding the properties of the slope materials of the Plio-Pleistocene age exposed in the hilly areas of the south-eastern part of Bangladesh. Furthermore, the results of the slope materials' index and shear strength properties will be helpful for future numerical modelling of slope stability, land use and utility planning, rainfall threshold determination and selection of landslide preventive and mitigation measures.

Declarations

Conflict of interest   The authors declare no competing interests.

References

Ahmed B (2021) The root causes of landslide vulnerability in Bangladesh. Landslides 8(5):1707–1720. https://doi.org/10.1007/s10346-020-01606-0

Ahmed B (2015) Landslide susceptibility modelling applying user-defined weighting and data-driven statistical techniques in Cox's Bazar Municipality, Bangladesh. Nat Hazards 79:1707–1737. https://doi.org/10.1007/s11069-015-1922-4

Ahmed B, Rahman MS, Sammonds P, Islam R, Uddin K (2020) Application of geospatial technologies in developing a dynamic landslide early warning system in a humanitarian context: the Rohingya refugee crisis in Cox's Bazar, Bangladesh. Geomat Nat Haz Risk 11:446–468. https://doi.org/10.1080/19475705.2020.1730988

Alam A, Sammonds P, Ahmed B (2020) Cyclone risk assessment of the Cox's Bazar District and Rohingya refugee camps in southeast Bangladesh. Sci Total Environ 704:135360. https://doi.org/10.1016/j.scitotenv.2019.135360

ASTM (2020a) ASTM Volume 04.08: Soil and Rock (I): D420 – D5876/D5876m. West Conshohocken, PA, USA: American Society for Testing and Materials

ASTM (2020b) ASTM Volume 04.09: Soil and Rock (II): D5878 – Latest. West Conshohocken, PA, USA: American Society for Testing and Materials

Bloom PR (2020) Soil pH and pH Buffering. In P. Huang, Y. Li & M. Sumner, Handbook of Soil Sciences (Two Volume Set) (2nd ed.). Boca Raton: CRC Press. Retrieved from https://doi.org/10.1201/b16386

Braun A, Fakhri F, Hochschild V (2019) Refugee camp monitoring and environmental change assessment of Kutupalong, Bangladesh, based on radar imagery of Sentinel-1 and ALOS-2. Remote Sens 11:1–34. https://doi.org/10.3390/rs11172047

CDMP-II (2012) Landslide Inventory and Landuse Mapping, DEM Preparation, Precipitation Threshold Value and Establishment of Early Warning Device. Dhaka, Bangladesh: Comprehensive Disaster Management Programme-II (CDMP-II); Ministry of Food and Disaster Management (MoFDM), Disaster Management and Relief Division (DMRD), Government of the People's Republic of Bangladesh

Curray JR (2005) Tectonics and history of the Andaman Sea region. J Asian Earth Sci 25:187–232. https://doi.org/10.1016/j.jseaes.2004.09.001

Davison L, Springman S (2000) Basic mechanics of soils. http://environment.uwe.ac.uk/geocal/SoilMech/basic/stiffness.htm. Accessed 17 Feb 2021

Fort M, Cossart E, Arnaud-Fassetta G (2010) Catastrophic landslides and sedimentary budgets. In: Goudie AS, Alcántara-Ayala I (eds) Geomorphological hazards and disaster prevention. Cambridge University Press, Cambridge, pp 75–86

GoB-UNHCR (2021) Document - Joint Government of Bangladesh - UNHCR population factsheet as of 28 February 2021. https://data2.unhcr.org/en/documents/details/85395. Accessed 11 Apr 2021

Gui Y, Zhang Q, Qin X, Wang J (2021) Influence of organic matter content on engineering properties of clays. Adv Civ Eng 2021:6654121. https://doi.org/10.1155/2021/6654121

Hasan ME, Zhang L, Dewan A, Guo H, Mahmood R (2020) Spatiotemporal pattern of forest degradation and loss of ecosystem function associated with Rohingya influx: a geospatial approach. L Degrad Dev. https://doi.org/10.1002/ldr.3821

Highland LM, Bobrowsky P (2008) The landslide handbook - a guide to understanding landslides. US Geol Surv Circ 1–147. https://doi.org/10.3133/cir1325

Hillier S (2009) Quantitative analysis of clay and other minerals in sandstones by X-ray powder diffraction (XRPD). In: Clay mineral cements in sandstones. Blackwell Publishing Ltd., pp 213–251. https://doi.org/10.1002/9781444304336.ch11

Hoogsteen MJJ, Lantinga EA, Bakker EJ, Groot JCJ, Tittonell PA (2015) Estimating soil organic carbon through loss on ignition: effects of

ignition conditions and structural water loss. Eur J Soil Sci 66:320–328. https://doi.org/10.1111/ejss.12224

Hossain F, Moniruzzaman DM (2021) Environmental change detection through remote sensing technique: a study of Rohingya refugee camp area (Ukhia and Teknaf sub-district), Cox's Bazar. Bangladesh Environ Challenges 2:100024. https://doi.org/10.1016/j.envc.2021.100024

ISCG (2020) Monsoon response in Rohingya refugee camps | 12 June to 15 October 2020 |HumanitarianResponse.https://www.humanitarianresponse.info/en/operations/bangladesh/document/monsoon-response-rohingya-refugee-camps-12-june-15-october-2020. Accessed 24 Jan 2021

Ito A, Wagai R (2017) Global distribution of clay-size minerals on land surface for biogeochemical and climatological studies. Sci Data 4:1–11. https://doi.org/10.1038/sdata.2017.103

Kariuki PC, van der Meer F (2004) A unified swelling potential index for expansive soils. Eng Geol 72:1–8. https://doi.org/10.1016/S0013-7952(03)00159-5

Michel J, Dario C, Marc-Henri D, Thierry O, Ivanna Marina P, Bejamin R (2020) A review of methods used to estimate initial landslide failure surface depths and volumes. Eng Geol 267:105478. https://doi.org/10.1016/j.enggeo.2020.105478

Persits F, Wandrey C, Milici R, Manwar A (2001) Digital geologic and geophysical data of Bangladesh: U.S. Geological Survey Open-File Report 97-470-H. USGS. Retrieved from https://doi.org/10.3133/ofr97470H

Prakasam C, Aravinth R, Nagarajan B, Kanwar VS (2020) Site-specific geological and geotechnical investigation of a debris landslide along unstable road cut slopes in the Himalayan region, India. Geomatics, Nat Hazards Risk 11:1827–1848. https://doi.org/10.1080/19475705.2020.1813812

Reimann K-U, Hiller K (1993) Geology of Bangladesh Schweizerbart'sche Verlagsbuchhandlung 1:1–92

Sultana N (2020) Analysis of landslide-induced fatalities and injuries in Bangladesh: 2000–2018. Cogent Soc Sci 6:1737402. https://doi.org/10.1080/23311886.2020.1737402

Tehrani F, Husken L (2019) Landslide susceptibility mapping of refugee camps in Bangladesh. In: Proceedings of the International Conference on Natural Hazards and Infrastructure. National Technical University of Athens

Townsend FC (1985) Geotechnical characteristics of residual soils. J Geotech Eng 111:77–94

Uyeturk CE, Huvaj N, Bayraktaroglu H, Huseyinpasaoglu M (2020) Geotechnical characteristics of residual soils in rainfall-triggered landslides in Rize. Turkey Eng Geol 264:105318. https://doi.org/10.1016/j.enggeo.2019.105318

Wagner JF (2013) Mechanical properties of clays and clay minerals. In: Developments in clay science. Elsevier B.V., pp 347–381

Zaman S, Sammonds P, Ahmed B, Rahman T (2020) Disaster risk reduction in conflict contexts: lessons learned from the lived experiences of Rohingya refugees in Cox's Bazar Bangladesh. Int J Disaster Risk Reduct 50. https://doi.org/10.1016/j.catena.2019.104093

Zhan J, Wang Q, Zhang W, Shangguan Y, Song S, Chen J (2019) Soil-engineering properties and failure mechanisms of shallow landslides in soft-rock materials. CATENA 181:104093. https://doi.org/10.1016/j.catena.2019.104093

A. S. M. Maksud Kamal · Farhad Hossain · Md. Zillur Rahman
Department of Disaster Science and Management (DSM), University of Dhaka, Dhaka 1000, Bangladesh

Bayes Ahmed (✉) · Peter Sammonds
Institute for Risk and Disaster Reduction (IRDR), University College London (UCL), Gower Street, London WC1E 6BT, UK
Email: bayes.ahmed@ucl.ac.uk